Published in final edited form as:
J Mech Behav Biomed Mater. 2012 February ; 6C: 9–20. doi:10.1016/j.jmbbm.2011.09.007.

Laser Processed TiN Reinforced Ti6Al4V Composite Coatings

Vamsi Krishna Balla[1,2], **Abhimanyu Bhat**[1,3], **Susmita Bose**[1], and **Amit Bandyopadhyay**[1,*]
[1]W. M. Keck Biomedical Materials Research Laboratory, School of Mechanical and Materials Engineering, Washington State University, Pullman, WA 99164, USA

Abstract

The purpose of this first generation investigation is to evaluate fabrication, *in vitro* cytotoxicity, cell-materials interactions and tribological performance of TiN particle reinforced Ti6Al4V composite coatings for potential wear resistant load bearing implant applications. The microstructural analysis of the composites was performed using scanning electron microscope and phase analysis was done with X-ray diffraction. *In vitro* cell-materials interactions, using human fetal osteoblast cell line, have been assessed on these composite coatings and compared with Ti6Al4V alloy control samples. The tribological performance of the coatings were evaluated, in simulated body fluids, up to 1000 m sliding distance under 10N normal load. The results show that the composite coatings contain distinct TiN particles embedded in α + β phase matrix. The average top surface hardness of Ti6Al4V alloy increased from 394 ± 8 HV to 1138 ± 61 HV with 40 wt.% TiN reinforcement. Among the composite coatings, the coatings reinforced with 40 wt. % TiN exhibited the highest wear resistance of 3.74×10^{-6} mm^3/Nm, which is lower than the wear rate, 1.04×10^{-5} mm^3/Nm, of laser processed CoCrMo alloy tested under identical experimental conditions. *In vitro* biocompatibility study showed that these composite coatings were non-toxic and provides superior cell-material interactions compared to Ti6Al4V control, as a result of their high surface energy. In summary, excellent *in vitro* wear resistance and biocompatibility of present laser processed TiN reinforced Ti6Al4V alloy composite coatings clearly show their potential as wear resistant contact surfaces for load bearing implant applications.

Keywords

Ti6Al4V; TiN; metal matrix composites; laser deposition; laser engineered net shaping; *in vitro* wear resistance; biocompatibility

1. Introduction

Pure titanium (Ti) and its alloys such as Ti6Al4V are widely used as load bearing implant materials because of their excellent biocompatibility and corrosion resistance (Geetha et al., 2000). However, their use in articulating components of the hip and knee prosthesis is limited due to their poor tribological properties (Geetha et al., 2000; Buchhanan et al., 1987). The wear debris generated due to poor wear resistance of Ti and its alloys results in

*Corresponding Author: Tel: 509-335-4862, Fax: 509-335-4662, amitband@wsu.edu.
[2]Current address: Central Glass and Ceramic Research Institute, Kolkata 700032, India.
[3]Current address: Advanced Manufacturing Center, Cockrell School of Engineering, The University of Texas at Austin, Austin, TX 78712.

osteolysis (Jasty, 1993), which is one of the main limiting factors affecting the long-term stability of load bearing implants (McGee et al., 2000; Edidin et al., 2001). Therefore, several surface modification techniques have been developed to improve the tribological properties of Ti and its alloys. These techniques include thermal oxidation (Dong and Bell, 2000), diamond like carbon coatings (Saikko et al., 2001), nitrogen diffusion hardening (Rodriguez et al., 1998), and titanium nitride (TiN) coatings (Pappas et al. 1995; Ward et al., 1998). Apart from high hardness and superior wear resistance of TiN coatings (Pappas et al. 1995; Ward et al., 1998; Torregrosa et al., 1995; Raimondi and Pietrabissa, 2000), the intrinsic biocompatibility and high corrosion resistance in the *in vivo* physiological environment make TiN based coatings/materials as an excellent choice for load bearing metal implants (Raimondi and Pietrabissa, 2000; Piscanec et al., 2004; Dion et al., 1993; Narayan et al., 1994; Sathish et al., 2010; Gutmanas and Gotman, 2004; Geetha et al., 2004). Moreover, the observed properties of TiN are not affected by sterilization (Raimondi and Pietrabissa, 2000; Piscanec et al., 2004; Hubler, 1999) and the adsorption of periprosthetic fluid protein such as albumin is also high on TiN (Serro et al., 2009). These TiN surface layers have been fabricated by a variety of methods including ion-implantation, physical vapor deposition (PVD), chemical vapor deposition (CVD), plasma nitriding, powder immersion reaction assisted coating, nitriding and laser gas nitriding (LGN). Laser nitriding (Sathish et al., 2010) has been found to result in good bonding with the substrate leading to superior interfacial properties than other techniques. Still, TiN monolithic coatings have found little application in the field of load bearing implants due to their inherent brittleness and catastrophic fracture possibilities. It has also been reported that TiN coatings are often prone to develop several problems *in vivo* (Ward et al., 1998; Raimondi and Pietrabissa, 2000; Harman et al., 1997).

It is known that the metal matrix composites (MMCs) reinforced with hard particles exhibit superior properties compared to their monolithic counterparts such as high fracture toughness, mechanical strength and wear resistance. Therefore, Ti or Ti alloy reinforced with TiN particle can potentially obviate the above problems associated with monolithic TiN coatings for load bearing implant applications. However, there has been very little reported literature available on fabrication of TiN reinforced Ti alloys (Romero et al., 2007a, 2007b). Earlier works on TiN reinforced Ti composited fabricated using conventional power metallurgical route although showed some improvement in mechanical and wear properties, the resultant composites were found to exhibit considerable amount of residual porosity (Romero et al., 2007a, 2007b). Therefore, in this first generation work, we explored the possibility of processing TiN reinforced Ti6Al4V alloy matrix composite coatings on commercially pure (CP) Ti substrate using Laser Engineered Net Shaping (LENS™) – a laser based additive manufacturing technology. Although Ti6Al4V alloy is currently being in use for load bearing implants such as hip and knee, based on our prior experience with laser processing, we believe that the use of CP Ti as a substrate will not have any significant influence on composite coating characteristics and/or properties. By exploiting capabilities such as layer-by-layer deposition and fabricating parts directly from a CAD file, it is possible to fabricate complex shaped MMC parts with novel designs and functional gradation in composition using LENS™. In this article, we report microstructural, *in vitro* tribological and biocompatibility properties of laser processed Ti6Al4V alloy composite coatings reinforced with 5 to 40 wt.% of TiN.

2. Experimental

2.1 Fabrication

Ti6Al4V alloy powder (Advanced Specialty Metals Inc., NH, USA) and TiN powder (Atlantic Equipment Engineers, NJ, USA) with particle size range between 50-150 μm and 45-75 μm, respectively were used as feedstock materials. The Ti6Al4V alloy powder and

TiNs were dry mixed in a metallic container using a twin-roller mixer at 60 rpm for 2h. Then the premixed powder was immediately poured into the powder feeder of the Laser Engineered Net Shaping (LENS™) system and the composites were deposited. Premixed powder with varying concentrations of TiN (0, 10, 15, 20 and 40 wt.%) were used to prepare Ti6Al4V alloy composite coatings. A LENS™-750 (Optomec Inc. Albuquerque, NM) equipped with a 500W continuous wave Nd:YAG laser was used to make ~ 3 mm thick coatings of ϕ 10 mm and 15 mm square samples on 3 mm thick commercially pure Ti substrate. For comparison, Ti6Al4V alloy deposits without TiN reinforcement were also prepared. Detailed description and capabilities of the LENS™ process can be found elsewhere (Bandyopadhyay et al., 2009; Balla et al., 2009a; Balla et al., 2008). Laser power, scan-speed and powder feed rate were optimized from multiple experiments carried out using laser powers between 250 and 450 W with scan speeds between 5 and 20 mm/s and powder feed rate between 15 and 30 g/min. Our initial experiments showed that complete melting of powder was achieved only at a laser powders greater than 350 W. Parts processed at lower laser powers resulted in severe porosity. Similar observations were made when high scan speeds and high powder feed rates were used during deposition. It was found that laser deposition carried out at a laser power level of 350 W, scan speed of 10 mm/s and powder feed rate of 15 g/min was suitable for these composite coatings. All the coatings were fabricated in a glove box containing an argon atmosphere with O_2 content less than 10 ppm to limit the oxidation of the alloy during processing. The disc samples were used for microstructural, hardness and *in vitro* cell-materials interactions study, and square samples were used for *in vitro* wear resistance evaluation. For *in vitro* wear rate comparison, medical grade CoCrMo alloy samples (15 × 15 mm, 2 mm thick) were also made at 450 W laser power, 22.5 mm/s scan speed and 46.5 g/min feed rate (Dittrick et al., 2011).

2.2 Microstructures, Phase Analysis and Hardness

Lasers processed Ti6Al4V alloy coatings with and without TiN were sectioned and mounted for metallographic analysis. The polished surfaces of the samples were cleaned and then etched with Kroll's reagent to reveal the microstructural features. Microstructural characterization of the composite samples was carried out using a field emission scanning electron microscope (FEI-SIRION, 200F). Constituent phases in the composite samples were identified using a Siemens D 500 Kristalloflex diffractometer with Cu Kα radiation (1.54056Å) at 20kV between the 2θ range of 30 and 90 degrees, and compared with those of as-received powders. Vickers microhardness measurements (Shimadzu, HMV-2) were made on these samples using a 1000 g load for 15 s and an average value of 20 measurements was reported. In order to track the microstructural/compositional variation across the deposit, a series of microhardness indentations were placed from one end of the deposit to the other end with neighboring indents being separated by 0.12 mm using Vickers microhardness tester at 300 g load applied for 15 s.

2.3 Contact Angles and Surface Energy

The surface energy of laser processed Ti6Al4V alloy coatings with and without TiN reinforcement was calculated from experimentally determined contact angles. The surfaces of the samples for contact angle measurements were ground using a series of SiC grinding papers with various sizes up to 1200 grit. Ground samples were then polished on a velvet cloth using a series of Al_2O_3 powders up to 0.05 μm suspended in distilled water. Finally, just before testing, all the samples were ultrasonically cleaned in an alcohol bath. This procedure ensured identical surface roughness and topography on all sample surfaces. Contact angles were measured using the sessile drop method with a face contact angle setup equipped with a microscope and a camera. Images were collected with the camera and the contact angle between the drop and the substrate was measured from the magnified image. For each sample and liquid combination, an average of 6 measurements is reported. Surface

energy of TiN coated Ti6Al4V samples were calculated based on contact angle measurements, which were conducted with two liquids with polar and non-polar characteristics: distilled water and diiodomethane. In this study, Fowkes' equation was used to calculate the energy (Owens and Wendt, 1969):

$$\frac{\gamma_L(1+Cos\theta)}{2} = \sqrt{\gamma_L^d \gamma_S^d} + \sqrt{\gamma_L^p \gamma_S^p} \quad (1)$$

$$\gamma_S = \gamma_S^d + \gamma_S^p \quad (2)$$

where, γ_s is the total surface energy of solid, γ_L is the total surface tension of liquid, γ_s^d and γ_s^p are respectively the dispersive and polar components of the solid surface energy.

2.4 In vitro Bone Cell-Materials Interactions

In vitro cytotoxicity behavior of composite coatings and Ti6Al4V alloy was evaluated for 3 and 5 day culture periods using human fetal osteoblast cell (hFOB) line (CRL-11372, ATCC, VA, USA). Each sample (3 samples for each composition and culture duration) was sterilized by autoclaving at 121°C for 20 min prior to cell culture experiment. Following this, cells were seeded onto sample surfaces, placed in a 6-well plate. 4 ml of DMEM cell media enriched with 10% fetal bovine serum was added to each well. Cultures were maintained in an incubator at 37°C under an atmosphere of 5% CO_2 and 95% air. The culture media were changed every alternate day.

Cell morphology on test samples was assessed after 3 and 5 days of incubation period using SEM. Cultured samples for SEM observation were rinsed with 0.1 M phosphate-buffered saline (PBS) and fixed with 2% paraformaldehyde/2% glutaraldehyde in 0.1 M cacodylate buffer overnight at 4°C. Following this, post fixation for each sample was made with 2% Osmium tetroxide (OsO_4) for 2h at room temperature. Fixed samples were then dehydrated in an ethanol series 30%, 50%, 70%, 95% and 100% three times, each followed by a hexamethyldisilane (HMDS) drying procedure. Dried samples were then mounted on aluminum stubs, gold coated and observed under an FESEM.

2.5 In vitro Tribological Properties

Linear reciprocating ball-on-disc wear testing, according to ASTM G133, was performed using a tribometer (NANOVEA, Microphotonics Inc., CA, USA) with ϕ 3 mm Al_2O_3 ball rubbing against Ti6Al4V alloy coatings with varying concentrations of TiN and laser processed CoCrMo alloy samples for comparison. The top surface of the samples were ground using a series of SiC grinding papers with various sizes up to 1200 grit. Samples were then polished on velvet cloth using a series of Al_2O_3 powder up to 1μm suspended in distilled water. Finally, just before wear testing, all the samples were ultrasonically cleaned in an alcohol bath. In all wear experiments, a constant linear oscillatory motion of 10 mm in length (the full cycle represents 20 mm of travel) with a constant speed of 2100 mm/min and constant normal load of 10 N were used. The wear rate of each test samples was calculated as mm^3/Nm for 1000 m of sliding distance. All tests were carried out in aseptic condition in freshly prepared simulated body fluid (SBF) at 37°C. We have selected SBF as a test medium based on several earlier reports, where SBF has been used as an articulating media to simulate wear on joint replacement devices (Dittrick et al., 2011; Sheejaa, et al., 2001; Bodhak et al., 2011; Balla et al., 2009b). Although the addition of proteins to SBF can change the wear behavior, present wear tests in SBF can also quantify the response of these

articulating surfaces under present experimental loading conditions. The ionic concentrations of the SBF used in present study are as follows: 2.5mM of Ca^{2+}, 1.5mM of Mg^{2+}, 142.0mM of Na^{+}, 5.0 mM of K^{+}, 147.8 mM of Cl^{-}, 4.2 mM of HCO^{3-}, 1.0 mM of $HPO4^{2-}$, 0.5 mM of $SO4^{2-}$.

3. Results and Discussion

3.1. Microstructures and Phase Analysis

Typical microstructural features of laser processed Ti6Al4V alloy and its composites reinforced with TiN are shown in Fig. 1. All samples were observed to be free from any gross defects such as porosity and cracks. However, the Ti6Al4V alloy composites with 40 wt.% TiN showed some chipped off TiN particles presumably occurred during grinding and polishing. Distinct TiN particles, which survived melting during deposition, were also observed in the microstructures of composite samples and no interfacial porosity was observed throughout the composite coating regions. Cross-sectional microstructures of the composite coatings (Fig. 1b and c) showed no evidence of interfacial defects/cracks suggesting excellent interfacial bonding with the substrate and between individual layers. It is known that laser processing yield good metallurgical bonding between the coating and the substrate due to complete melting during micro-casting of individual layers (Sathish et al., 2010; Dittrick et al., 2011; Balla et al., 2009b; Nwobu et al., 1999; Selamat et al., 2001; Bell et al., 1986; Kloosterman and De Hosson, 1995). Further, it is intuitive to expect superior adhesion/bond strength for the present laser processed coatings, because of complete melting and subsequent solidification of materials at the interface, than those processed via plasma processing where the bonding is due to solid state diffusion (Roy et al., 2011). High magnification FESEM microstructures of laser processed composites are compared with pure Ti6Al4V alloy in Fig. 2. Pure Ti6Al4V alloy exhibited a typical α + β microstructures with relatively large prior β grain size as shown in Fig. 2a. However, the composites showed relatively fine β grain structure with large amount of acicular α phase (Fig. 2b and c). Further, it appears that finer TiN powder dissolved in the alloy matrix and reprecipitated as fine particles, which can be clearly seen in the composite coatings with 20 and 40% TiN as shown in Figs. 2c and d. Although none of the composite coating samples showed the presence of gross porosity, it is quite normal to expect some fine residual pores in LENS™ processed materials.

The formation of microstructural features during laser processing of TiN reinforced Ti6Al4V alloy composites is not known. However, microstructures formed during laser surface nitriding of CP Ti and Ti6Al4V alloy in an atmosphere containing varying concentrations of N_2 have been studied (Nwobu et al., 1999; Selamat et al., 2001; Bell et al., 1986; Kloosterman and De Hosson, 1995; Walker et al., 1985; Kechemair et al., 1992). These earlier investigations show that the presence/formation of TiN in the CP Ti and Ti6Al4V alloy during laser nitriding increases the laser absorbptivity, as a result the peak melt pool temperatures, under identical laser parameters, increased from ~ 2100°C to ~ 3100°C for CP Ti (Nwobu et al., 1999). Therefore, under present experimental conditions of 350 W compared to 204 W in earlier work (Nwobu et al., 1999), it is expected that the melt pool temperatures can exceed the melting temperatures of Ti6Al4V alloy (1604 to 1660°C) and can reach temperatures above 3100°C. Such a high melt pool temperatures can melt fine fraction of TiN particles (melting point between 2930 and 3290°C) in these composites. Such high temperature rise in LENS™ is not uncommon since we routinely produce Ta parts using LENS™ where the melting temperature is >3100°C. Figs. 3a and b shows the reaction layers formed between TiN particles and Ti6Al4V alloy matrix. It can be seen that the reaction layer was relatively thin around coarse TiN particles (Fig. 3a) compared to finer TiN particles (Fig. 3b). These microstructural observations indicate clear interaction between the TiN particles and the Ti6Al4V alloy matrix during laser processing. Further, the

finer fraction of TiN could completely melt under present experimental conditions resulting in fine TiN precipitates in the matrix as shown in Fig. 2d. Since, the LENS™ process is characterized by rapid cooling rates, of the order of 10^3 to 10^5 K/s, there will be very little time for the N to escape from the metal. Therefore, TiN particles reprecipitate from the supersaturated metal, which were found to be high in the regions where the partially melted TiN particles were closely spaced. This is presumably due to rapid enrichment of surrounding matrix with nitrogen as a result of closely spaced neighboring reaction zones around TiN. In the other regions where the reaction layers around the TiN are further apart and do not impinge on each other, the dissolved nitrogen (due to complete or partial melting of TiN particles) in the open Ti6Al4V alloy melt pool resulted in the formation of needle like α phase (martensite), as shown in Fig. 3c. The formation of needle like α martensite in the present composite coatings is attributed to rapid cooling rates associated with the laser processing and also due to the stabilizing effect of dissolved nitrogen in the alloy matrix (Wriedt and Murray, 1987). Similar microstructural features were also observed in laser nitrided Ti and Ti6Al4V alloy (Sathish et al., 2010; Nwobu et al., 1999; Selamat et al., 2001; Bell et al., 1986; Kloosterman and De Hosson, 1995; Walker et al., 1985; Kechemair et al., 1992). X-ray diffraction (XRD) analysis of laser processed Ti6Al4V alloy composite coatings reinforced with TiN clearly showed the presence of TiN, α and β phases, as shown in Fig. 4. Since the deposition was carried out in an argon atmosphere with oxygen content less than 10 ppm, none of the samples showed the presence of any oxide peaks. As expected the intensity of TiN peaks increased with increasing concentration of TiN in the composite coatings. The XRD results obtained on these composite coatings corroborate with microstructural observations as discussed above.

3.2. In vitro Bone Cell-Materials Interactions

In vitro cell-materials interactions with hFOB cells showed high concentration of cells, at all culture durations, with relatively high coverage of the surface and confluent layer on TiN reinforced composite coatings compared to laser processed Ti6Al4V alloy control samples suggesting their non toxicity and superior biocompatibility than Ti6Al4V alloy. Since the cell growth is clear on these substrates, it is certain that even standard MTT assay will show an increase in living cell density as a function of time. In Fig. 5, sample surfaces imaged after 3 days of culture to investigate hFOB bone cell attachment, and spreading on different surfaces are shown. Among the surfaces, fewer cells were observed on laser processed Ti6Al4V alloy samples (Fig. 5a) compared to the samples with TiN reinforcement. Further, on the TiN reinforced composite sample surfaces hFOB cells were found to spread and well attached to the surface (Figs. 5b-d). However, on pure Ti6Al4V alloy fewer cells were observed and with rounded morphology. It is known that osteoblasts are attachment-dependant cells and therefore they must attach first on the surface then spread and mineralize their extracellular matrix. The cell density was also observed to increase with an increase in the concentration of TiN. Bone cells formed a confluent layer covering the entire surface of composites with 40% TiN as shown in Fig. 5d. Dense growth of cells on the composites surface with numerous cell-cell contacts clearly suggests that these surfaces are biocompatible and provide superior surfaces for bone cell adhesion and growth than Ti6Al4V alloy. Interestingly, the formation of small white granular apatite nodules on cell surface (Figs. 5c and b) was also observed on these TiN coated surfaces. FESEM images of samples cultured for 5 days are presented in Fig. 6 to show the cell proliferation. On composite surfaces, cells formed a confluent layer covering the entire surface as shown in Figs. 6b-d. Cells are seen to adhere to each other with cellular micro extensions and connected to substrate in addition to the neighboring cells (Fig. 6b). However, on Ti6Al4V alloy surfaces without TiN the cell growth was observed to be significantly less pronounced in comparison to composite surfaces. From Fig. 6c and d, it can be seen that cells have already started to mineralize their extracellular matrix with the abundance deposition of

apatite minerals. Presence of apatite on *in vitro* cultured samples has also been confirmed in earlier works (Bodhak et al., 2011; Das et al., 2008) based on SEM morphological observations similar to those shown in Figs. 5c, d and 6c, d.

The cell attachment and growth are primarily associated with material's chemistry and surface characteristics such as roughness, wettability and surface energy. Since all the samples used in the present work were prepared following identical grinding and polishing procedure, we hypothesize that the cellular activities on these samples are more of materialistic phenomenon than due to surface roughness. Recently, it has also been reported that the surface energy is a more influential surface characteristic on cellular adhesion and proliferation (Bodhak et al., 2009; Hallab et al., 2001) for high surface energy materials such as metals and ceramics compared to low surface energy polymers. In addition, enhancing the polar component of the surface energy via compositional or surface modifications is also shown to enhance cellular adhesion and proliferation (Redey et al., 1999; Feng et al., 2003). Therefore, all samples have been characterized in terms of polar and dispersive components and total surface energy. The experimental results shown in Table 1 indicate a relatively lower contact angles for composite samples than for pure Ti6Al4V, thus improving the wettability of these composites. Since the cell media are water based, the cellular attachment will be poor on any hydrophobic surface with high contact angle. Moreover, a low contact angle of composite surfaces suggests high surface energy, which is another factor that can contribute to better cell attachment (Bodhak et al., 2009; Hallab et al., 2001). Table 1 also shows different components of surface energy of Ti6Al4V alloy with and without TiN. All composites showed significantly higher surface energy than the surface energy of pure Ti6Al4V alloy, which is consistent with the observed cell-materials interactions of these samples. The surface energy was also found to increase with increase in the TiN concentration in the composites. The total surface energy of the Ti6Al4V alloy increased from 50.55 ± 2.20 mN/m to 60.93 ± 1.88 mN/m when the alloy was reinforced with 40% TiN. The exact mechanism of improvement of cellular activity with TiN or N concentration in Ti and Ti6Al4V is not yet known. However, we hypothesize that the observed improvement in cellular adhesion and proliferation on composite samples is due to the positive influence of polar component of the surface energy (Redey et al., 1999; Feng et al., 2003), which is significantly higher (26.44 ± 2.66 mN/m) than that of pure Ti6Al4V alloy (14.42 ± 1.10 mN/m). In addition to the surface energy, the dissolution of nitrogen in the Ti6Al4V alloy matrix of composite coatings could also contribute to the superior cellular response on these surfaces compared to pure Ti6Al4V. In line with these variations, the nitrogen content of different TiN films found to affect the properties of cell adhesion on TiN coatings (Cyster et al., 2002). Present results show that the TiN reinforced Ti6Al4V alloy composites are non-toxic with improved cell-materials interactions than uncoated Ti6Al4V.

3.3 In vitro Wear Rate

In vitro wear rate, in mm^3/Nm, of laser processed Ti6Al4V and its composite coatings reinforced with varying amounts of TiN was calculated from the wear track dimensions measured using SEM images of the worn surfaces. Fig. 7 shows experimentally determined wear rate of laser processed Ti6Al4V and its composite coatings for a sliding distance of 1000 m. Experimental data clearly indicate that TiN reinforced Ti6Al4V alloy composite coatings has superior wear resistance compared to Ti6Al4V without TiN. The wear rate of pure Ti6Al4V was found to be 1.03×10^{-3} mm^3/Nm and it was decreased by an order of magnitude between 2.8×10^{-4} and 4.3×10^{-4} mm^3/Nm with addition of up to 20% TiN. Lowest wear rate was observed with Ti6Al4V alloy reinforced with 40% TiN which exhibited a wear rate of 3.74×10^{-6} mm^3/Nm. Moreover, the wear rate of composite coatings with 40% TiN was found to be lower than CoCrMo alloy (1.04×10^{-5} mm^3/Nm), which is currently used commercially for acetabular ball in hip implants. The wear rate of

the order of 10^{-6} mm^3Nm^{-1} observed for 40% TiN reinforced composite coatings is comparable to laser gas nitrided Ti (Sathish et al., 2010). However, as stated, present composites can have superior fracture toughness compared to monolithic TiN coatings produced by other techniques. Therefore, the present TiN reinforced Ti6Al4V composite coatings show higher wear resistance and have the potential to be used in wear resistant load bearing implant applications.

Table 2 show that the average top surface hardness of laser processed Ti6Al4V alloy with and without TiN. For comparison the hardness of laser processed CoCrMo alloy is also presented in Table 2. The average top surface hardness of composites ranged between 489 and 527 HV. These hardness values are significantly higher than the average hardness of the laser deposited Ti6Al4V, which was 394±8 HV. The average hardness of laser processed CoCrMo alloy (464 ± 4 HV) was comparable with composite coatings with 15% TiN. However, the wear rate of CoCrMo alloy was found to be lower than those observed for Ti6Al4V composites reinforced with TiN up to 20%. This difference is attributed to the variations in microstructural features of these materials. However, the composite coatings with 40% TiN showed highest hardness of 1138 ± 61 HV, which resulted in lower wear rate during *in vitro* wear testing in SBF. In order to track the microstructural variations across the deposit, a series of microhardness indent markers were placed from one end of the transition region to the other. The hardness profile across the coating thickness is shown in Fig. 8. The cross-sectional hardness of the coatings varied between 530 - 600 HV as a function of distance from the interface up to 1.5 mm. Therefore, the hardness data beyond 1.5 mm from the interface was not measured. The hardness profiles showed no significant improvement in the hardness with increasing concentration of TiN up to 20% TiN. The smooth nature of hardness profiles across the composite coatings indicates the absence of any gross defects such as cracks and pores in the coatings. The average top surface hardness of composites (Table 2) corresponds very well with the observed *in vitro* wear rates (Fig. 7). In addition to the reported hardness and *in vitro* wear rate, the fracture toughness of present composite coatings is also important for long-term *in vivo* stability. However, due to reinforcing effect of TiN particles the fracture toughness of composite coatings will always be higher than the substrate. Further, it is expected that the toughness mismatch between metal and metal matrix composites do not pose major problem as observed in metal-ceramic combinations.

Fig. 9 illustrates the worn surfaces of laser processed Ti6Al4V with and without TiN, and CoCrMo alloy after 1000 m of sliding in SBF. Evidently, evenly worn deep track with distinct grooves was observed on Ti6Al4V without TiN reinforcement, as shown in Fig. 9a. However, relatively shallow and smoother worn tracks were observed on Ti6Al4V composite coatings with 40% TiN (Fig. 9c) and CoCrMo alloy (Fig. 9d). No significant difference in wear tracks was observed between composite coatings with varying concentrations. However, the composites with low concentration of TiN showed relatively higher cracking and chipping of TiN particles, as shown in Fig. 9b, and the chipping decreased with increasing TiN concentration in the composite coatings (Fig. 9c). High magnification FESEM images of the worn tracks, shown in insets of Fig. 9, showed some parallel array of fatigue cracks oriented normal to the sliding direction and chipped off regions on Ti6Al4V alloy surface suggesting fatigue type wear. Often such tiny microcracks coalesce to form a longer cracks and result in chipped off regions on the surface as shown in Fig. 9a (inset). Although no visible fatigue cracks were observed on TiN reinforced Ti6Al4V alloy composite coatings, isolated cracking and chipping of the TiN particles was observed (Fig. 9c, **inset**). On CoCrMo alloy surface no such chipping was observed, Fig. 9d, and is attributed to the absence of any second phase reinforcing particles. None of the composite samples showed evidence of complete removal of TiN reinforcements from the coatings. This is an important observation, as earlier study (Sathish et al., 2010) on wear behavior of laser nitrided Ti and Ti alloys showed complete wear/removal of TiN dendrites

after 40,000 cycles (1200 m) under 10 N load. The inferior wear performance of laser nitrided coatings could be due to limited thickness of the hard TiN surface and presence of process induced minute cracks on the top surface (Sathish et al., 2010). Complete removal of hard and wear resistant phase from the top surface is detrimental to the long-term wear performance of load bearing metal implant. However, our *in vitro* wear results on laser processed TiN reinforced Ti6Al4V composite coatings suggest that present composites provide significantly better articulating surfaces for long-term stability of load bearing implants compared to laser nitrided monolithic TiN coatings on Ti and its alloys (Sathish et al., 2010). In summary, excellent *in vitro* wear resistance and biocompatibility of present laser processed TiN reinforced Ti6Al4V alloy composite coatings clearly show their potential as wear resistant contact surfaces for load bearing implant applications such as in acetabular ball and/or cup for hip prosthesis. However, further *in vivo* studies and long-term wear tests are needed on these materials to fully understand the tissue-materials interactions and wear mechanisms.

4. Conclusions

TiN reinforced Ti6Al4V alloy composite coatings were successfully fabricated using Laser Engineered Net Shaping (LENS™) – a laser based additive manufacturing technology. *In vitro* biocompatibility study using hFOB cells showed excellent biocompatibility and superior cell-materials interactions of TiN reinforced Ti6Al4V composite coatings compared to Ti6Al4V alloy. *In vitro* wear rate of these composite coatings was found to be in the range of 2.8×10^{-4} and 3.74×10^{-6} mm^3/Nm. Lowest wear rate was observed on Ti6Al4V alloy with 40 wt.% TiN (3.74×10^{-6} mm^3/Nm), which is lower than the wear rate of laser processed CoCrMo alloy (1.04×10^{-5} mm^3/Nm). Among the composite coatings, the coatings reinforced with 40 wt.% TiN exhibited the highest wear resistance and superior cell-materials interactions than pure Ti6Al4V.

Acknowledgments

Authors would like to acknowledge the financial support from the W. M. Keck Foundation to establish a Biomedical Materials Research Lab at WSU. Authors also acknowledge the financial support from the M. J. Murdock Charitable Trust, National Science Foundation NSF (Grant No. CMMI 0728348) and National Institutes of Health (Grant No. NIH-R01-EB-007351).

References

Geetha M, Singh AK, Asokamani R, Gogia AK. Ti based biomaterials, the ultimate choice for orthopedic implants – A review. Prog Mater Sci. 2009; 54:397–425.

Buchhanan RA, Regney, Williams JM. Wear-accelerated corrosion of Ti-6Al-4V and nitrogen-ion-implanted Ti-6Al-4V: Mechanisms and influence of fixed-stress magnitude. Biomed Mater Res. 1987; 21:367–377.

Jasty M. Clinical reviews: particulate debris and failure of total hip replacements. J Appl Biomater. 1993; 4:273–276. [PubMed: 10146311]

McGee MA, Howie DW, Costi K, Haynes DR, Wildenauer CI, Pearcy MJ. Implant retrieval studies of the wear and loosening of prosthetic joints: a review. Wear. 2000; 241:158–165.

Edidin AA, Rimnac CM, Goldberg VM, Kurtz SM. Mechanical behaviour, wear surface morphology, and clinical performance of UHMWPE acetabular components after 10 years of implantation. Wear. 2001; 250:152–158.

Dong H, Bell T. Enhanced wear resistance of titanium surfaces by a new thermal oxidation treatment. Wear. 2000; 238:131–137.

Saikko V, Ahlroos T, Calonius O, Keranen J. Wear simulation of total hip prostheses with polyethylene against CoCrMo, alumina and diamond-like carbon. Biomaterials. 2001; 22:1507–1514. [PubMed: 11374449]

Rodriguez D, Gil FJ, Planell JA. Wear resistance of the nitrogen diffusion hardening of the Ti6Al4V alloy. J Biomech. 1998; 31:49.

Pappas MJ, Makris G, Buechel FF. Titanium nitride ceramic film against polyethylene. A 48 million cycle wear test Clin Orthop. 1995; 317:64–70.

Ward LP, Subramanian C, Strafford KN, Wilks TP. Sliding wear studies of selected nitride coatings and their potential for long- term use in orthopaedic applications. Proc Inst Mech Eng [H]. 1998; 212:303–315.

Torregrosa F, Barrallier L, Roux L. Phase analysis, microhardness and tribological behaviour of Ti-6Al-4V after ion implantation of nitrogen in connection with its application for hip-joint prosthesis. Thin Solid Films. 1995; 266:245–253.

Raimondi MT, Pietrabissa R. The in-vivo wear performance of prosthetic femoral heads with titanium nitride coating. Biomaterials. 2000; 21:907–913. [PubMed: 10735467]

Piscanec S, Ciacchi LC, Vesselli E, Comelli G, Sbaizero O, Meriani S, De Vita A. Bioactivity of TiN-coated titanium implants. Acta Mater. 2004; 52:1237–1245.

Dion I, Rouais F, Trut L, Baquey C, Monties JR, Havlik P. TiN coating: surface characterization and haemocompatibility. Biomaterials. 1993; 14:169–176. [PubMed: 8476989]

Narayan J, Fan WD, Narayan RJ, Tiwari P, Stadelmaier HH. Diamond, diamond-like and titanium nitride biocompatible coatings for human body parts. Mat Sci Eng B. 1994; 25:5–10.

Sathish S, Geetha M, Pandey ND, Richard C, Asokamani R. Studies on the corrosion and wear behavior of the laser nitrided biomedical titanium and its alloys. Mater Sci Eng, C. 2010; 30:376–382.

Gutmanas EY, Gotman I. PIRAC Ti nitride coated Ti–6Al–4V head against UHMWPE acetabular cup–hip wear simulator study. J Mater Sci – Mater Med. 2004; 15:327–330. [PubMed: 15332594]

Geetha M, Mudali UK, Pandey ND, Asokamani R, Raj B. Microstructural and Corrosion Evaluation of Laser Surface Nitrided Ti-13Nb-13Zr Alloy. Surf Eng. 2004; 20:68–74.

Hubler R. Hardness and corrosion protection enhancement behaviour of surgical implant surfaces treated with ceramic thin films. Surf Coat Technol. 1999; 116:1111–1115.

Serro AP, Completo C, Colaço R, dos Santos F, Lobato da Silva C, Cabral JMS, Araújo H, Pires E, Saramago B. A comparative study of titanium nitrides, TiN, TiNbN and TiCN, as coatings for biomedical applications. Surf Coat Technol. 2009; 203:3701–3707.

Harman MK, Banks SA, Hodge WA. Wear analysis of a retrieved hip implant with titanium nitride coating. J Arthroplasty. 1997; 12-18:938–945. [PubMed: 9458260]

Romero F, Amigó V, Salvador MD, Vicente A. Interactions in titanium matrix composites reinforced by titanium compounds by conventional PM route. Mater Sci Forum. 2007a; 534-536:817–820.

Romero F, Amigó V, Salvador MD, Martinez E. Mechanical and microstructural properties of titanium matrix composites reinforced by TiN particles. Mater Sci Forum. 2007b; 534-536:825–828.

Bandyopadhyay A, Balla VK, Xue W, Bose S. Application of laser engineered net shaping (LENS) to manufacture porous and functionally graded structures for load bearing implants. J Mater Sci – Mater Med. 2009; 20:S29–S34. [PubMed: 18521725]

Balla VK, Bose S, Bandyopadhyay A. Fabrication of porous NiTi shape memory alloy structures using laser engineered net shaping. J Biomed Mater Res B. 2009a; 89B:481–490.

Balla VK, Xue W, Bose S, Bandyopadhyay A. Engineered porous metals for implants. JOM. 2008; 60(5):45–48.

Dittrick S, Balla VK, Davies NM, Bose S, Bandyopadhyay A. In vitro wear rate and Co ion release of compositionally and structurally graded CoCrMo-Ti6Al4V structures. Mater Sci Eng C. 2011; 31:809–814.

Owens DK, Wendt RC. Estimation of the surface free energy of polymers. J Appl Polym Sci. 1969; 13(8):1741–1747.

Sheejaa D, Taya BK, Laua SP, Nung LN. Tribological characterisation of diamond-like carbon coatings on Co–Cr–Mo alloy for orthopaedic applications. Surf Coat Technol. 2001; 146-147:410–416.

Bodhak S, Balla VK, Bose S, Bandyopadhyay A, Kashalikar U, Jha SK, Sastri S. In vitro biological and tribological properties of transparent magnesium aluminate (Spinel®) and aluminum oxynitride (AlON®). J Mater Sci – Mater Med. 2011 In press. 10.1007/s10856-011-4332-5

Balla VK, Xue W, Bose S, Bandyopadhyay A. Laser assisted Zr/ZrO_2 coating on Ti for load-bearing implants. Acta Biomater. 2009b; 5:2800–2809. [PubMed: 19398221]

Nwobu AIP, Rawlings RD, West DRF. Nitride formation in titanium based substrates during laser surface melting in nitrogen-argon atmospheres. Acta Mater. 1999; 47:631–643.

Selamat MS, Baker TN, Watson LM. Study of the surface layer formed by the laser processing of Ti-6Al-4V alloy in a dilute nitrogen environment. J Mater Proc Technol. 2001; 113:509–515.

Bell T, Bergmann H, Lanagan J, Morton PH, Staines AM. Surface engineering of titanium with nitrogen. Surf Eng. 1986; 2:133–143.

Kloosterman AB, De Hosson JThM. Microstructural characterization of laser nitrided titanium. Scripta Metall Mater. 1995; 33:567–573.

Mangal R, Balla VK, Bandyopadhyay A, Bose S. Compositionally Graded Hydroxyapatite / Tricalcium Phosphate Coating on Ti by Laser and Induction Plasma. Acta Biomater. 2011; 7:866–873. [PubMed: 20854939]

Walker A, Folkes J, Steen WM, West DRF. Laser surface alloying of titanium substrates with carbon and nitrogen. Surf Eng. 1985; 1:23–29.

Kechemair, D.; Laurens, P.; Sabatier, L.; Ricaud, JP. Proc Laser Advanced Mater Processing '92, Vol 1, High Temperature Soc of Japan, 1992. Matsunawa, A.; Katayama, S., editors. 1992. p. 281

Wriedt, HA.; Murray, JL. Phase diagrams of binary titanium alloys. ASM International, UAA; 1987. p. 176

Bodhak S, Bose S, Bandyopadhyay A. Role of surface charge and wettability on early stage mineralization and bone cell-materials interactions of polarized hydroxyapatite. Acta Biomater. 2009; 5:2178–2188. [PubMed: 19303377]

Hallab NJ, Bundy KJ, O'Connor K, Moses RL, Jacobs JJ. Evaluation of metallic and polymeric biomaterial surface energy and surface roughness characteristics for directed cell adhesion. Tissue Eng. 2001; 7:55–72. [PubMed: 11224924]

Redey SA, Razzouk S, Rey C, Bernache-Assollant D, Leroy G, Nardin M, Cournot G. Osteoclast adhesion and activity on synthetic hydroxyapatite, carbonated hydroxyapatite, and natural calcium carbonate: relationship to surface energies. J Biomed Mater Res. 1999; 45:140–147. [PubMed: 10397968]

Feng B, Weng J, Yang BC, Qu SX, Zhang XD. Characterization of surface oxide films on titanium and adhesion of osteoblast. Biomater. 2003; 24:4663–4670.

Cyster LA, Grant DM, Parker KG, Parker TL. The effect of surface chemistry and structure of titanium nitride (TiN) films on primary hippocampal cells. Biomol Eng. 2002; 19:171–175. [PubMed: 12202178]

Das K, Balla VK, Bandyopadhyay A. Surface Modification of Laser Processed Porous Titanium for Load Bearing Implants. Scripta Mater. 2008; 59:822–825.

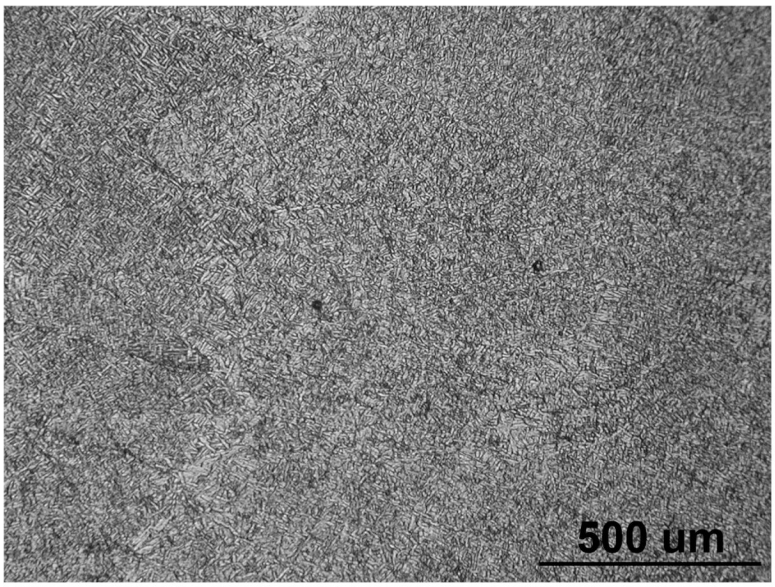

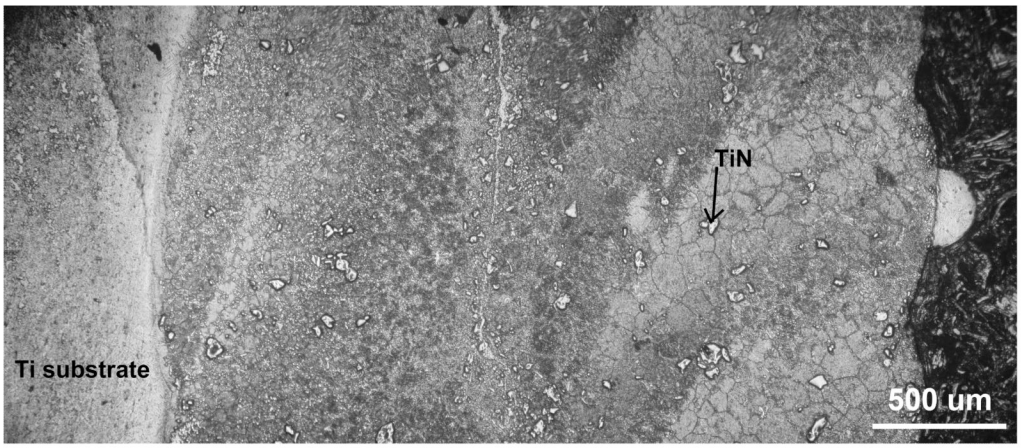

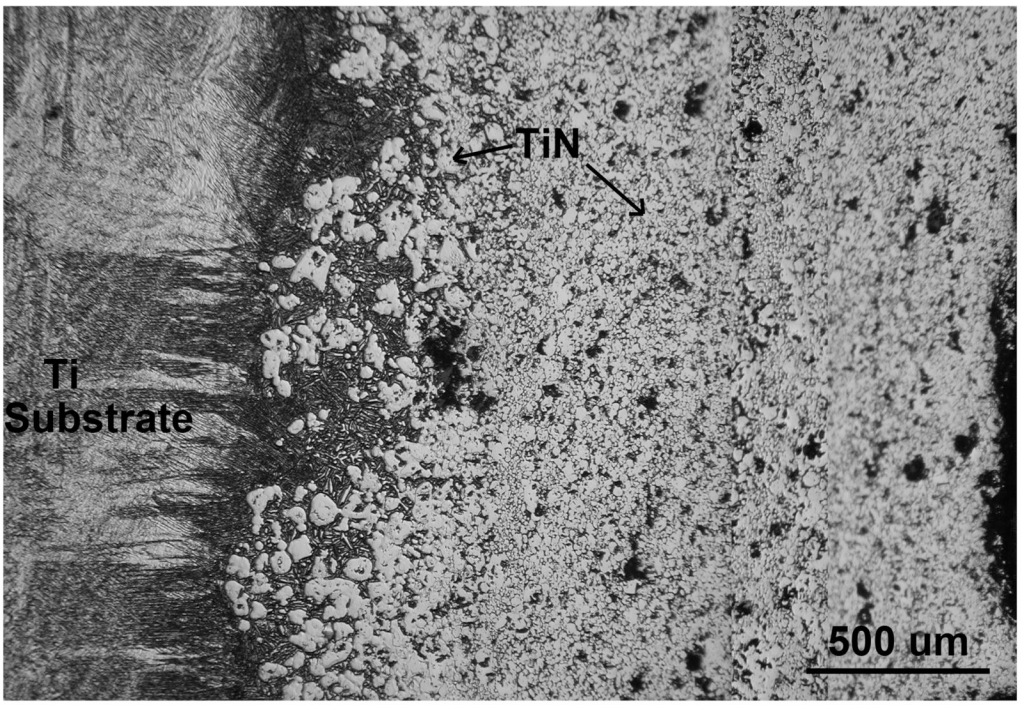

Fig. 1.
Typical cross-sectional microstructures of laser processed Ti6Al4V alloy and Ti6Al4V+TiN composites (a) Ti6Al4V alloy, (b) Ti6Al4V+10% TiN, (c) Ti6Al4V+40% TiN.

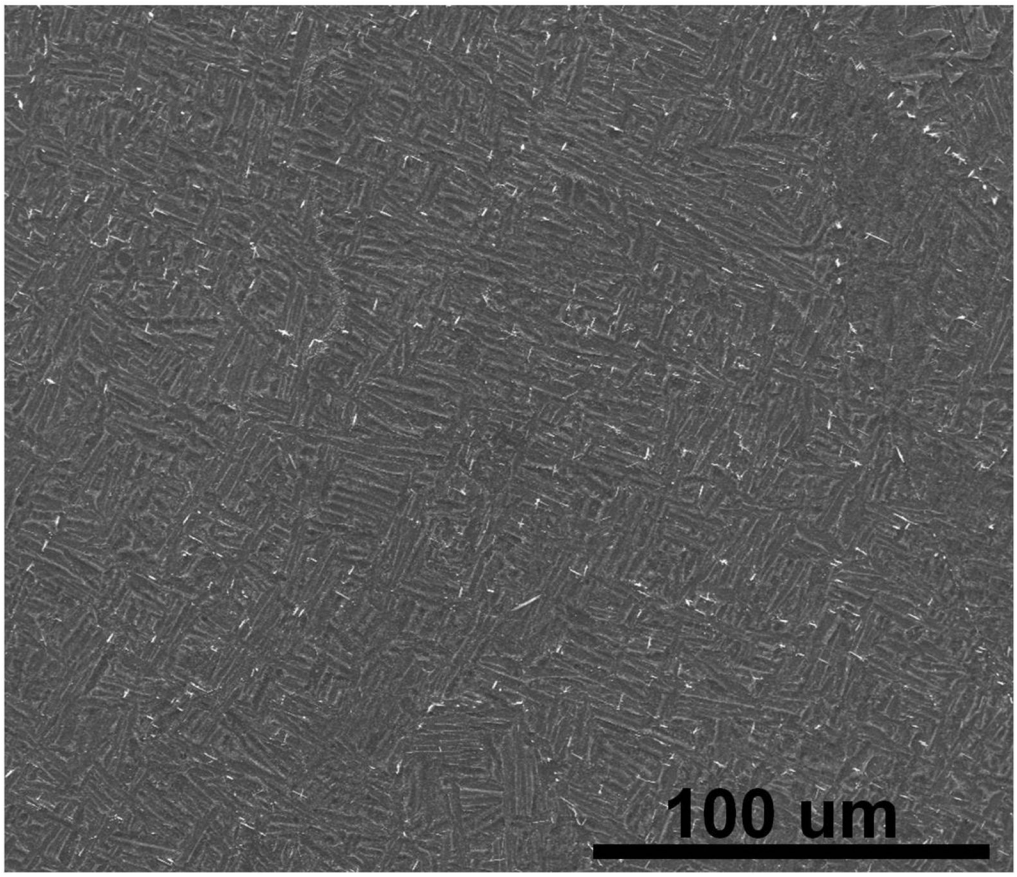

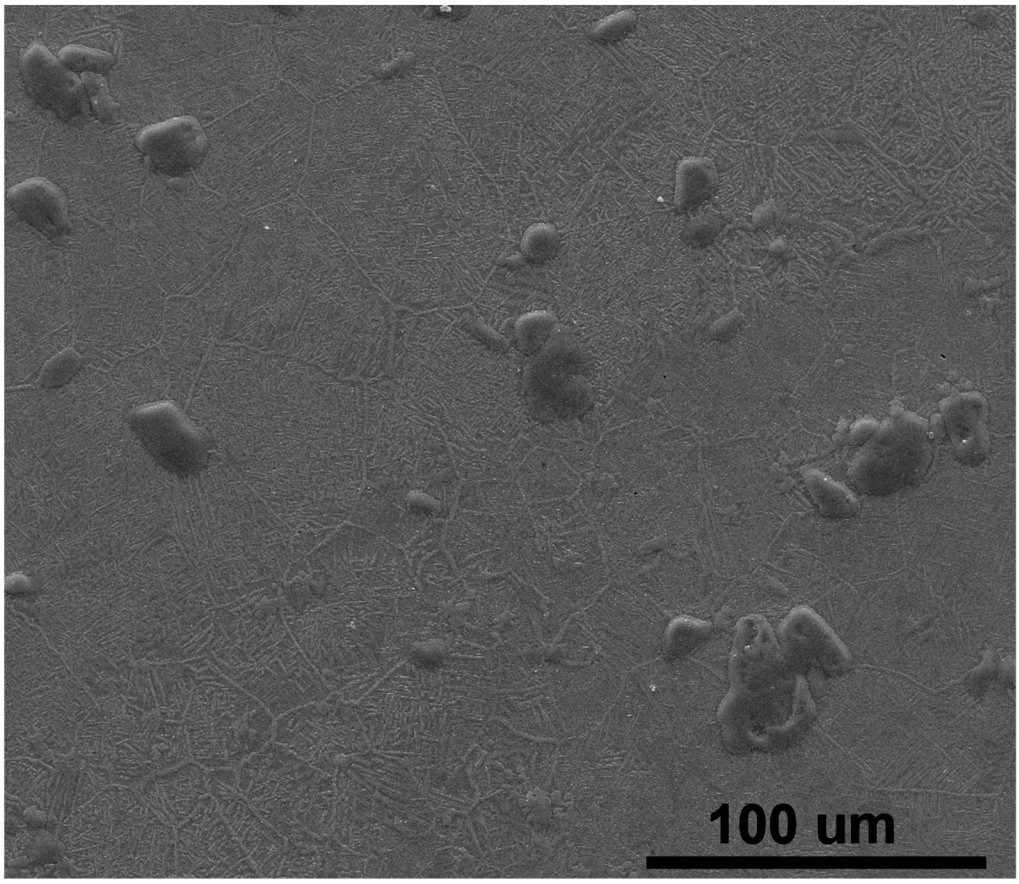

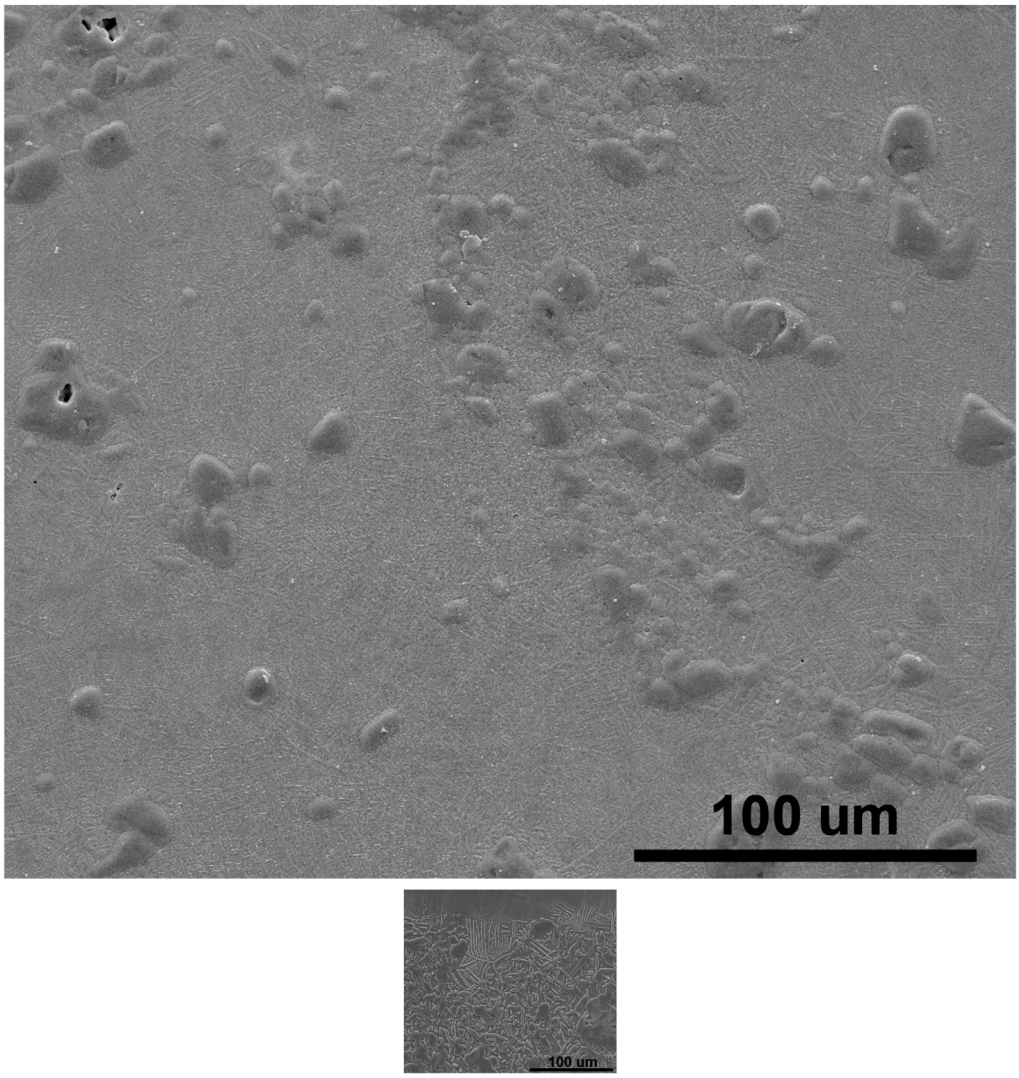

Fig. 2.
FESEM microstructures of laser processed (a) pure Ti6Al4V alloy, (b) Ti6Al4V+10%TiN composites (c) Ti6Al4V+20%TiN composites, (d) Ti6Al4V+40% TiN composites.

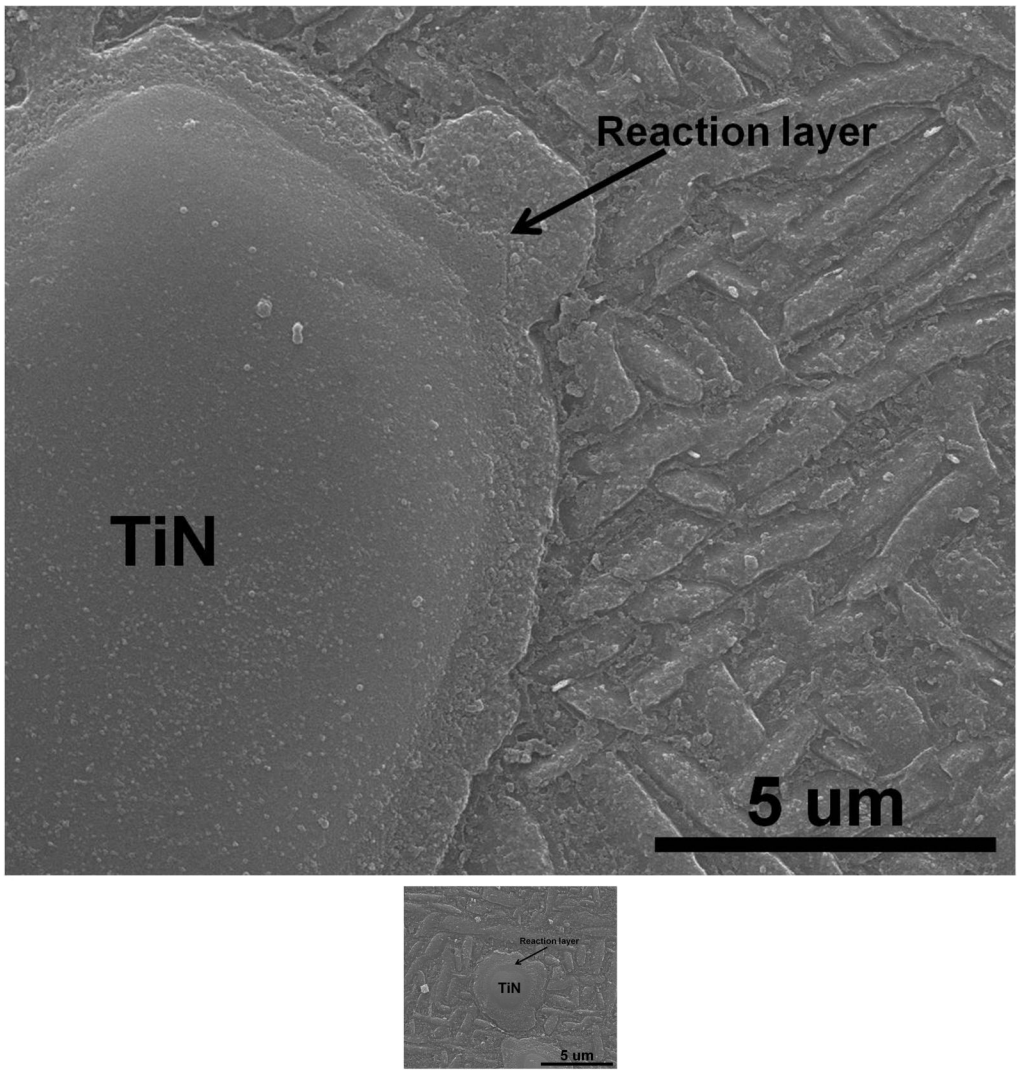

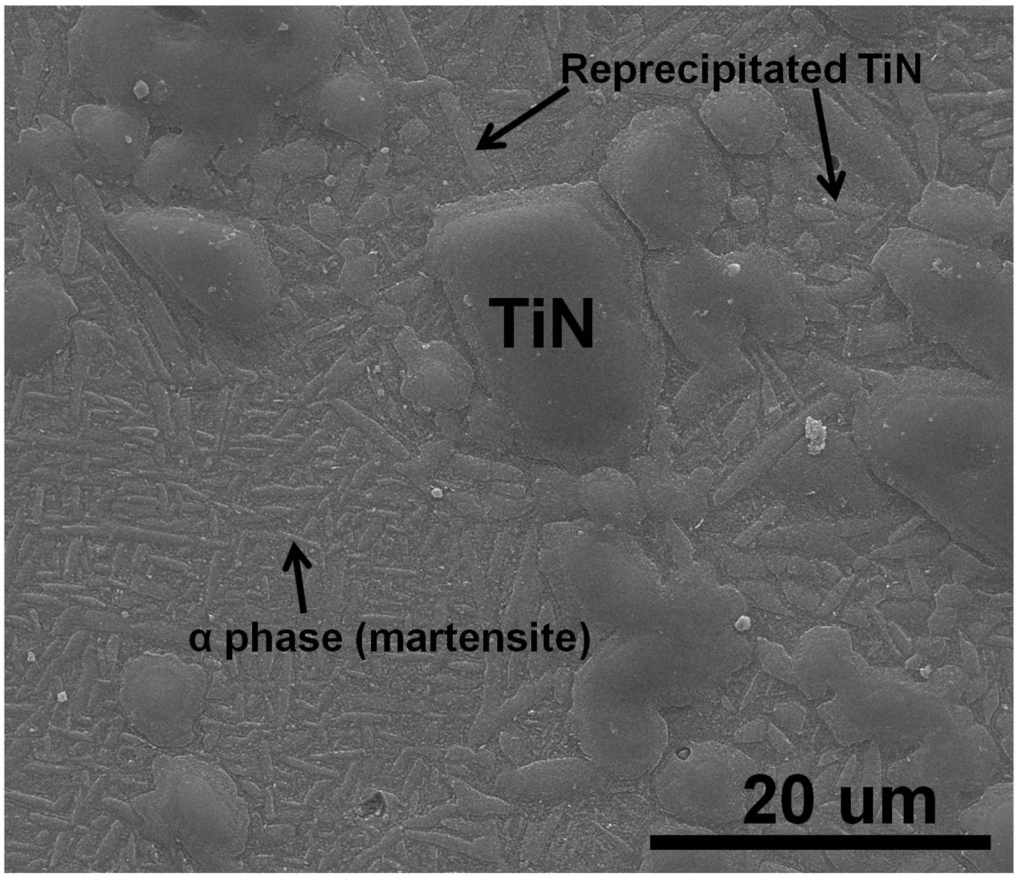

Fig. 3.

High magnification FESEM microstructures showing the reaction layers between TiN particles and Ti6Al4V alloy matrix (a) reaction layer between coarse TiN particle and the matrix in Ti6Al4V+10%TiN composite, (b) reaction layer between finer TiN particle and the matrix in Ti6Al4V+20%TiN composite, (c) microstructure of Ti6Al4V+20%TiN composite showing needle like α phase (martensite) in the regions with low concentration of TiN particles and reprecipitated TiN particle in the regions with high concentration of TiN particles.

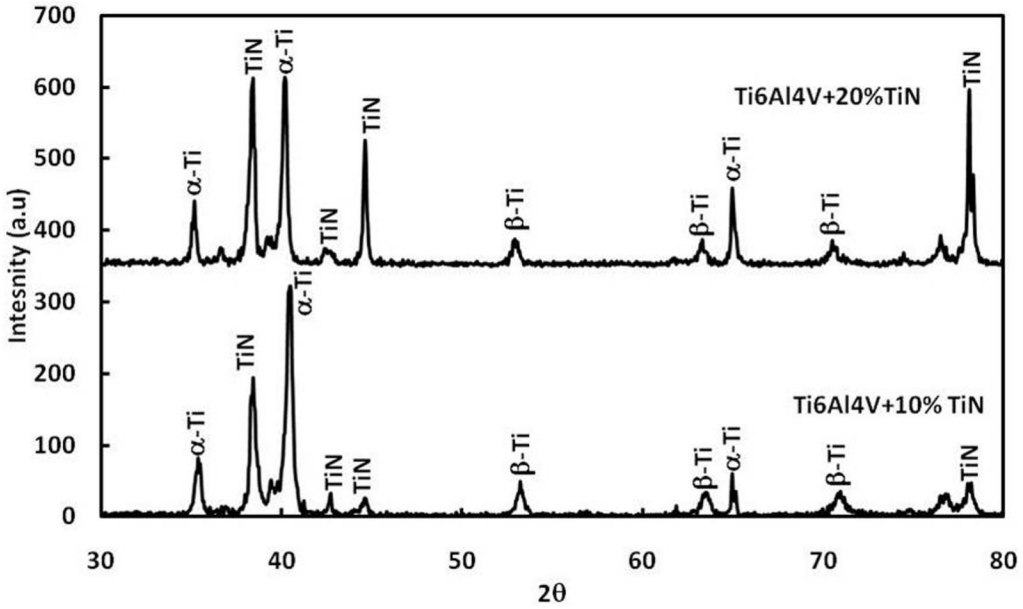

Fig. 4.
X-ray diffraction spectra of laser processed TiN reinforced Ti6Al4V alloy composite coatings.

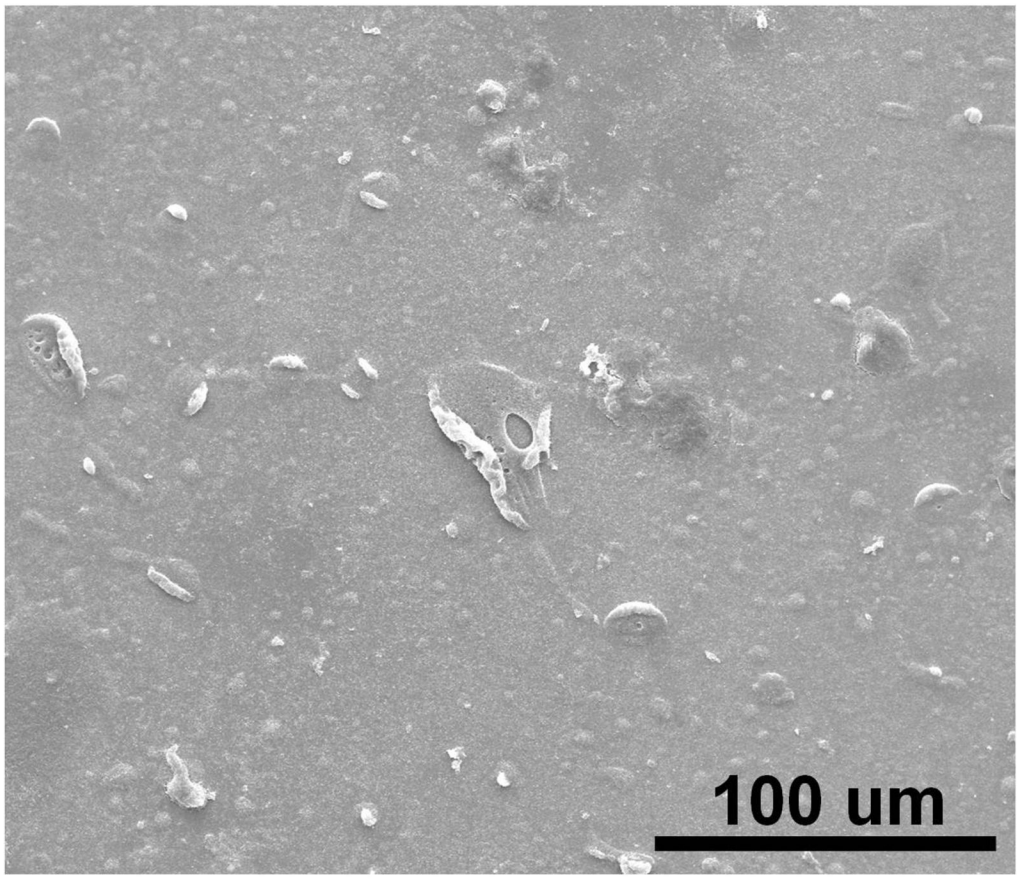

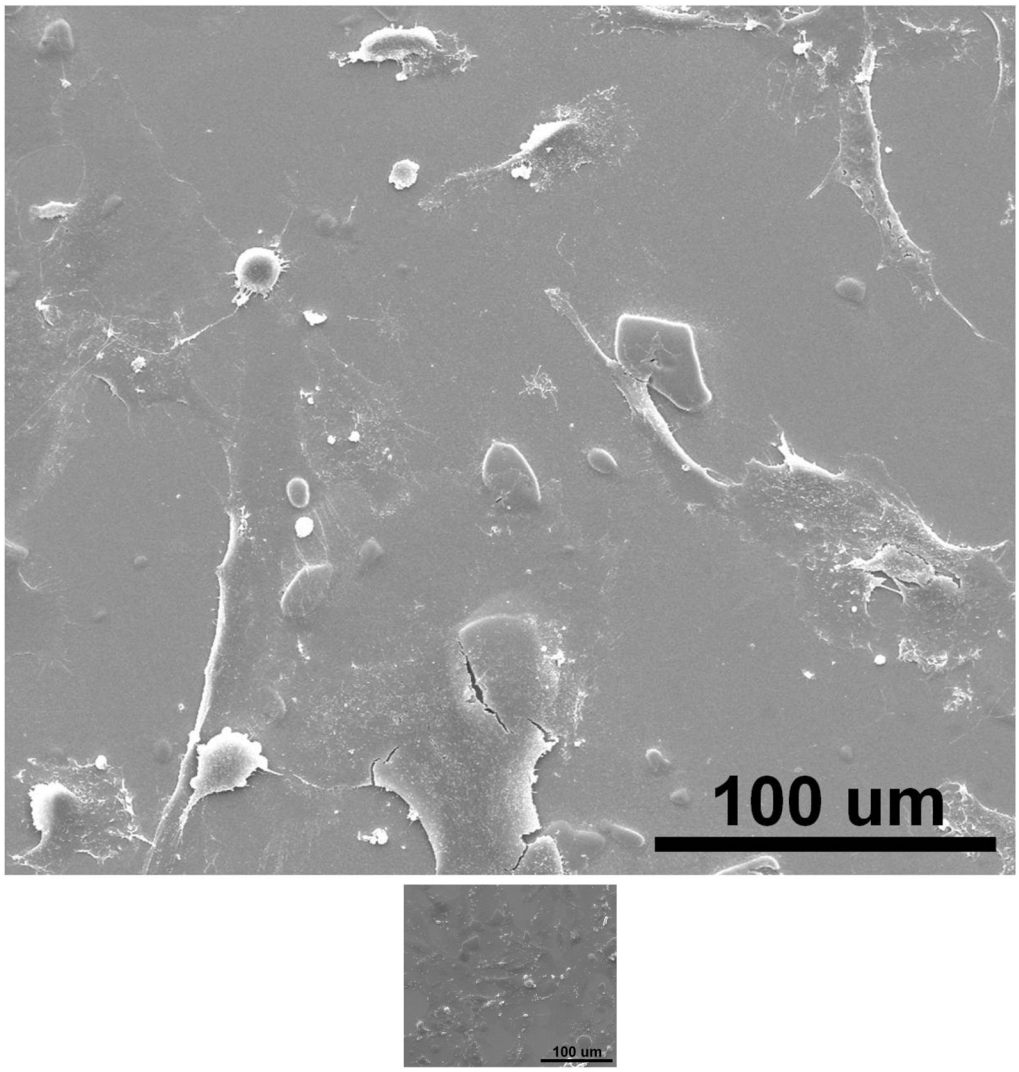

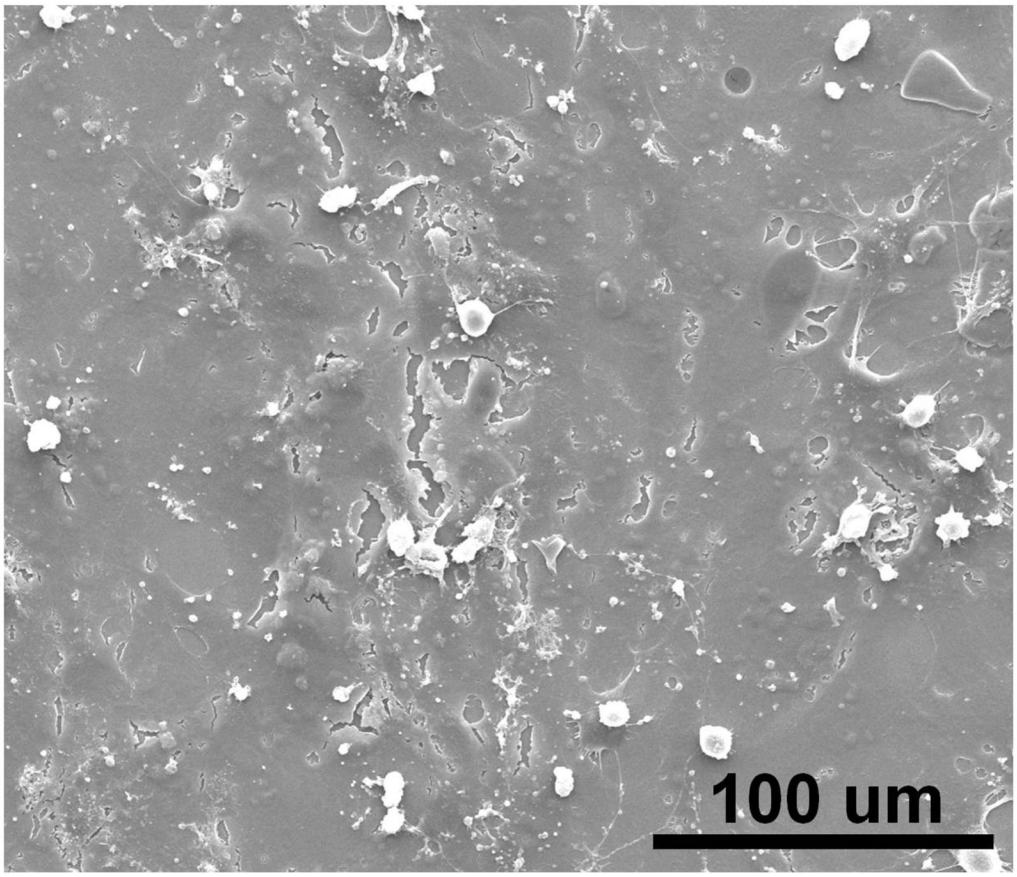

Fig. 5.
FESEM micrographs illustrating morphologies of hFOB cells adhered to different surfaces after 3 days of culture on (a) Ti6Al4V alloy, (b) Ti6Al4V+10% TiN, (c) Ti6Al4V+20% TiN, (d) Ti6Al4V+40% TiN.

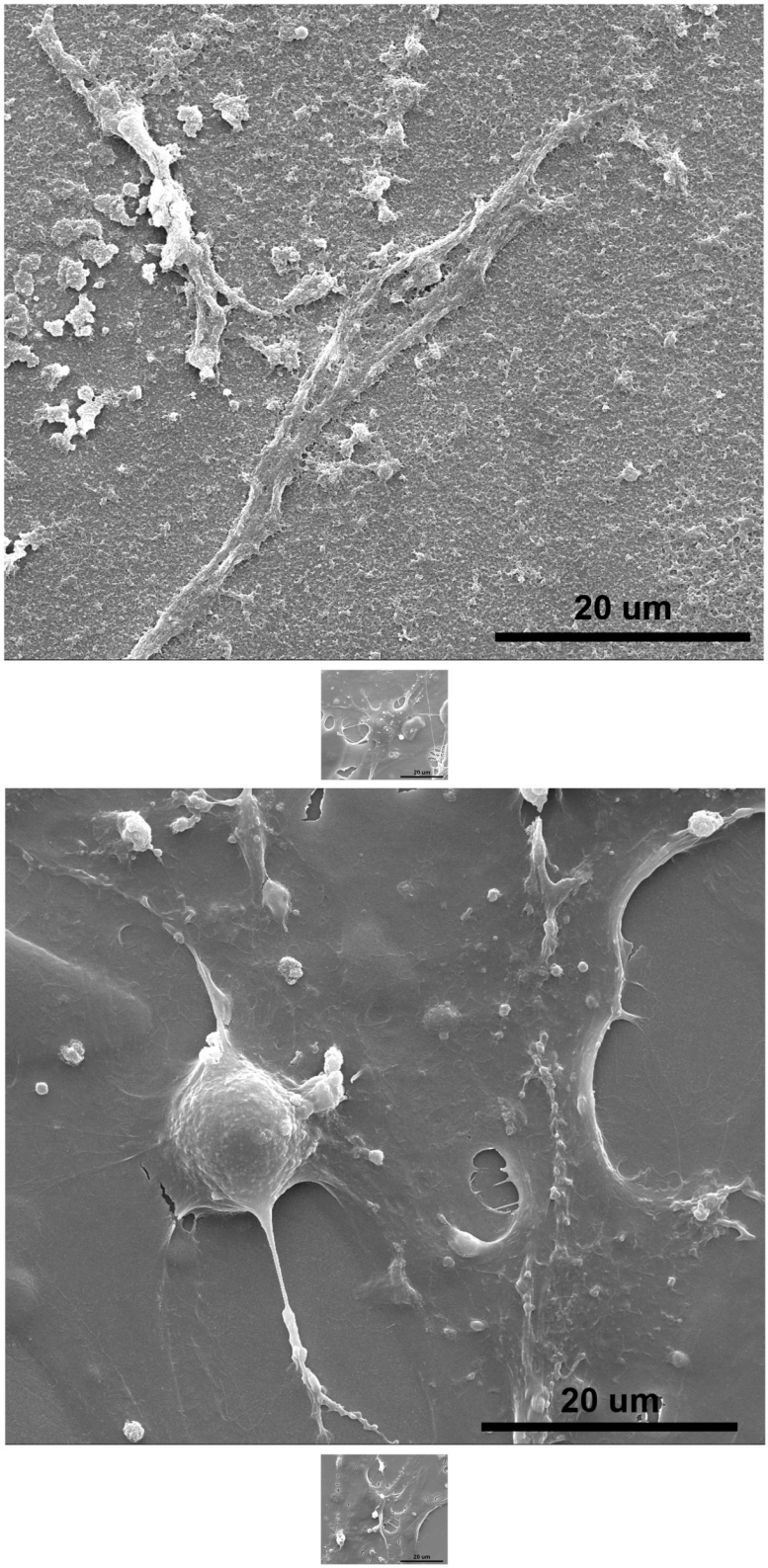

Fig. 6.

FESEM micrographs illustrating morphologies of hFOB cells after 5 days of culture on (a) Ti6Al4V alloy, (b) Ti6Al4V+10% TiN, (c) Ti6Al4V+20% TiN, (d) Ti6Al4V+40% TiN.

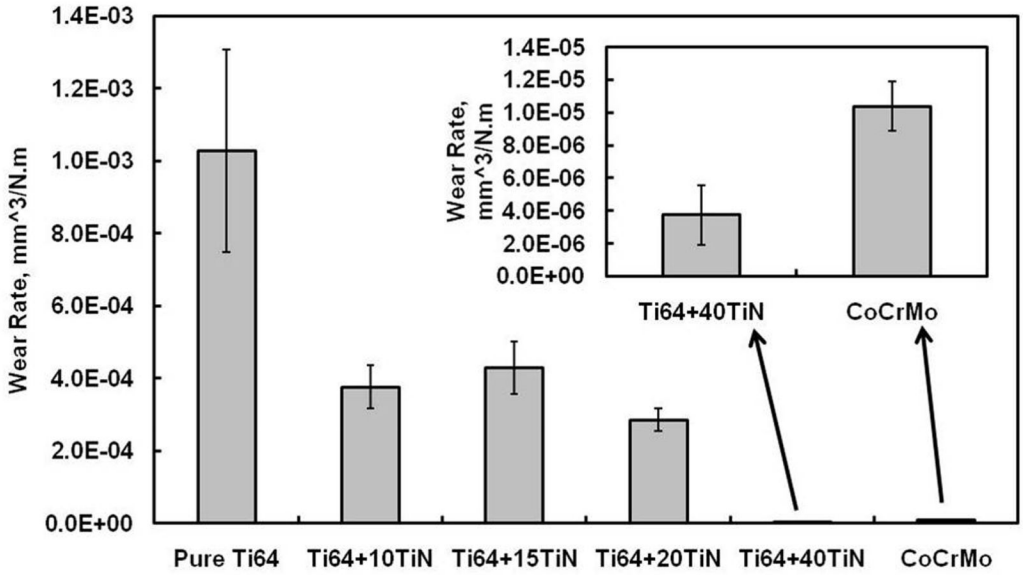

Fig. 7.

Wear rate of laser processed Ti6Al4V alloy (Ti64), CoCrMo alloy and Ti6Al4V alloy composites reinforced with varying concentrations of TiN.

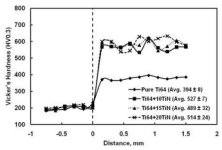

Fig. 8.
Hardness variation across the Ti6Al4V and Ti6Al4V+TiN composites.

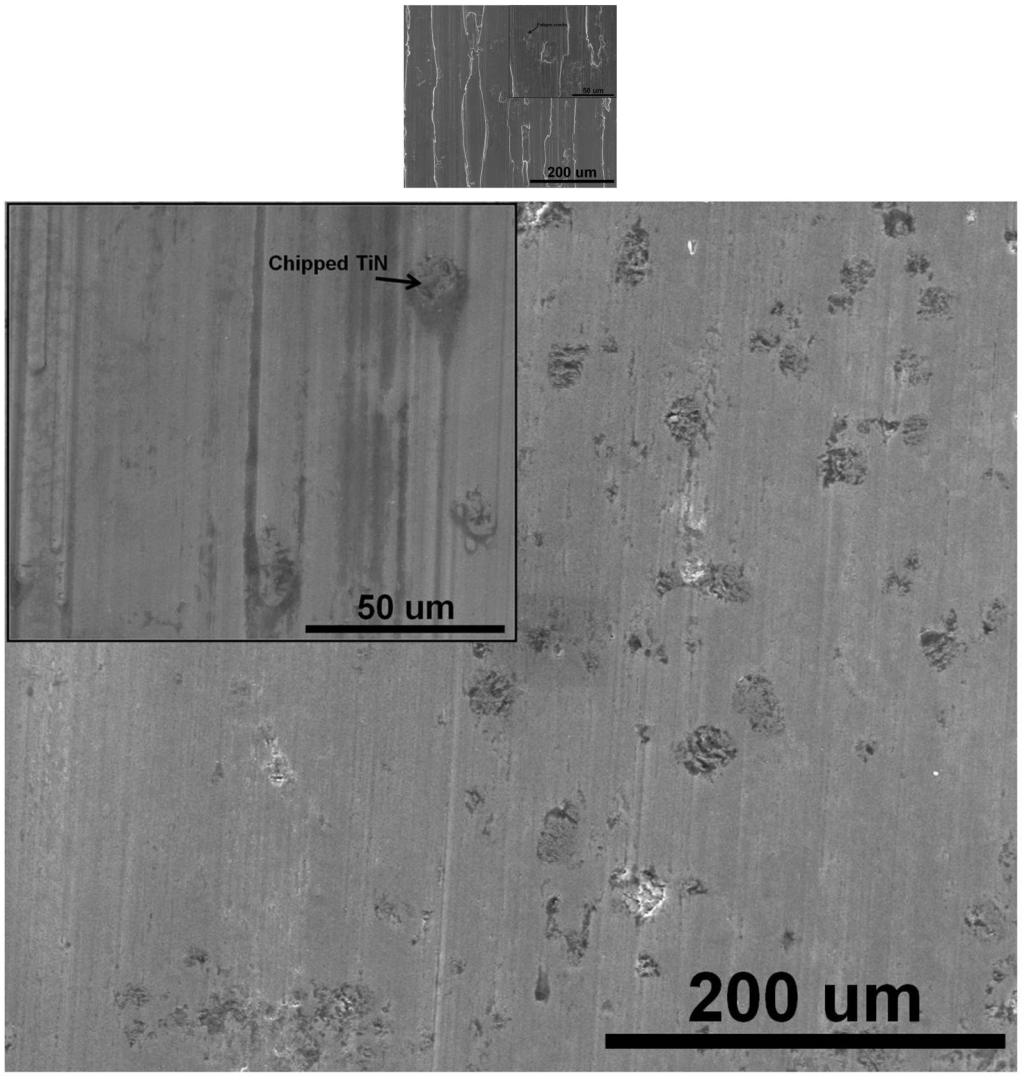

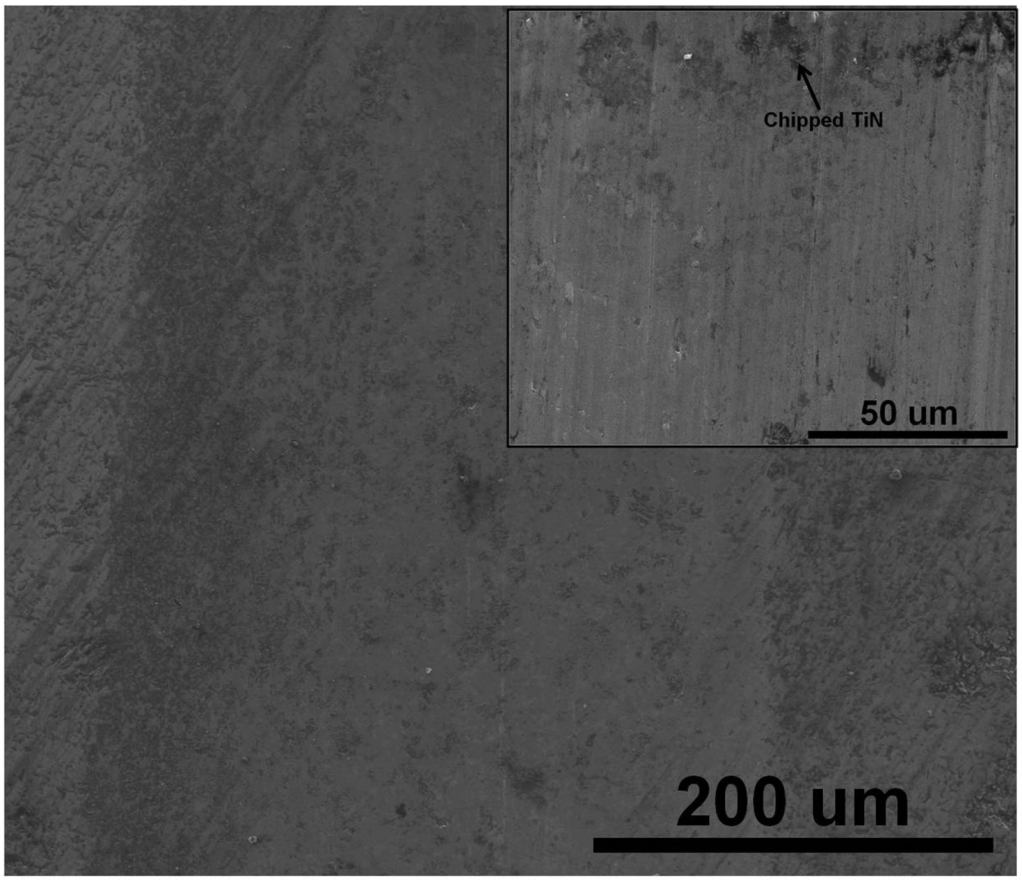

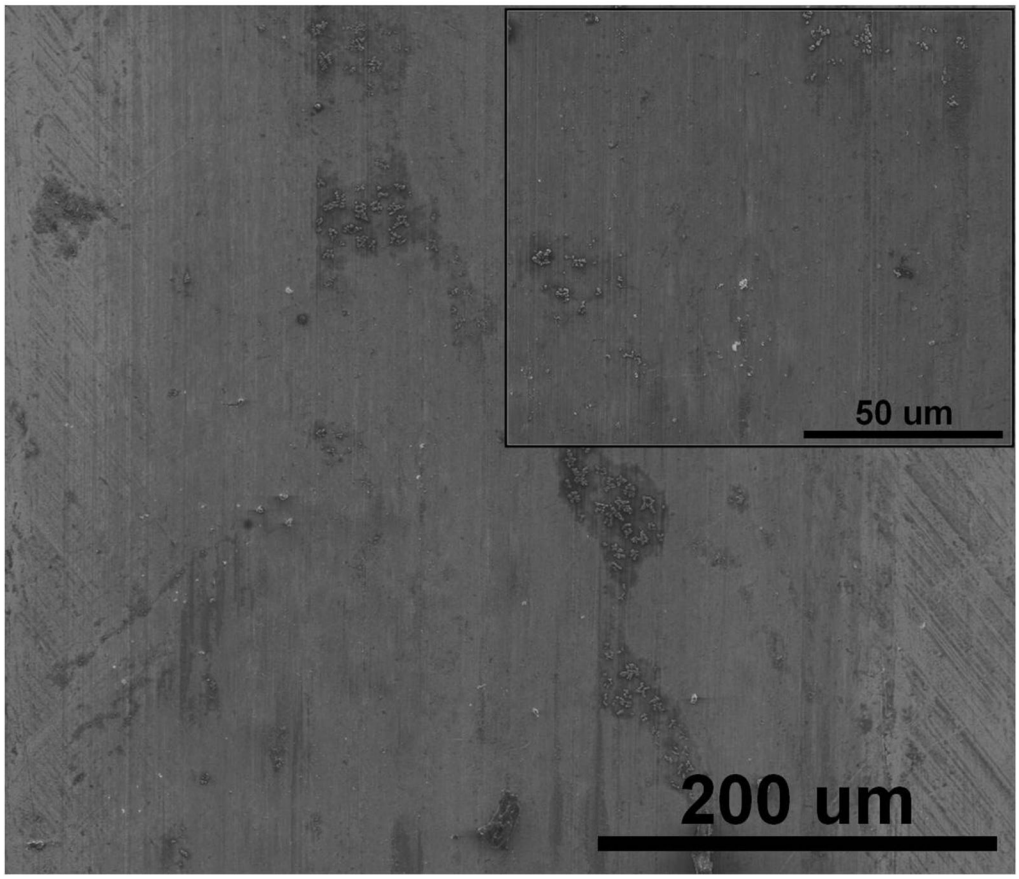

Fig. 9.
Wear track morphology after 1000 m of sliding distance (a) Ti6Al4V alloy, (b) Ti6Al4V +15% TiN, (c) Ti6Al4V+40% TiN, (d) CoCrMo alloy. Insets show high magnification FESEM images of respective wear tracks.

Table 1

Contact angles (°), polar and dispersive components of total surface energy (mN/m) of various surfaces.

Surface	DI water	Diiodomethane	γ^d	γ^p	Total Surface Energy
Pure Ti6Al4V	58.97 ± 2.39	46.6 ± 3.32	36.12 ± 1.81	14.42 ± 1.10	50.55 ± 2.20
Ti6Al4V +10%TiN	53.02 ± 6.56	40.73 ± 4.17	39.18 ± 2.13	16.70 ± 4.10	55.88 ± 3.44
Ti6Al4V +15%TiN	39.35 ± 3.49	47.58 ± 3.38	35.58 ± 1.83	26.44 ± 2.66	62.02 ± 1.69
Ti6Al4V +20%TiN	41.08 ± 5.58	44.67 ± 3.58	37.15 ± 1.92	24.54 ± 3.61	61.70 ± 3.12
Ti6Al4V +40%TiN	42.20 ± 3.12	45.3 ± 3.23	36.84 ± 1.42	24.08 ± 2.52	60.93 ± 1.88

J Mech Behav Biomed Mater. Author manuscript; available in PMC 2013 February 1.

Table 2

Top surface hardness (HV1.0) of laser processed Ti6Al4V alloy (Ti64), CoCrMo alloy and Ti6Al4V alloy composites reinforced with varying concentrations of TiN.

Material	Hardness
Pure Ti6Al4V	394 ± 8
Ti6Al4V +10%TiN	527 ± 7
Ti6Al4V +15%TiN	489 ± 31
Ti6Al4V +20%TiN	514 ± 24
Ti6Al4V +40%TiN	1138 ± 61
Pure CoCrMo	464 ± 4